Int. J. Heat Mass Transfer. Vol. 32, No. 6, pp. 1165–1174, 1989
Printed in Great Britain

0017–9310/89 $3.00+0.00

Thermal boundary condition effects on heat transfer in the turbulent incompressible flat plate boundary layer

ROBERT P. TAYLOR, HUGH W. COLEMAN, M. H. HOSNI
and PHILIP H. LOVE

Thermal & Fluid Dynamics Laboratory, Department of Mechanical and Nuclear Engineering, Mississippi State University, Mississippi State, MS 39762, U.S.A.

(*Received* 25 *July* 1988 *and in final form* 29 *November* 1988)

Abstract—Experimental Stanton number results are presented for the turbulent incompressible flat plate boundary layer with a variety of thermal boundary conditions—constant wall temperature, constant wall heat flux, and linear wall temperature variations. These experiments have extended the range of such heat transfer data to a Reynolds number, Re_x, of 10 000 000. The thermal boundary condition is found to have a significant influence on the behavior of the Stanton number. The experimental results are compared with the various heat transfer theories—analogies with skin friction, solutions of the integral boundary layer equations, and finite difference solutions of the Reynolds averaged boundary layer equations.

INTRODUCTION

TURBULENT incompressible flat plate boundary layer flow is one of the fundamental problems of convective heat transfer and is of great academic and practical interest. Therefore, it is, next to pipe flow, the most studied and best understood turbulent flow and heat transfer problem. However, there is still a dearth of heat transfer data. To our knowledge, all of the data is limited to values of $Re_x < 3.5 \times 10^6$ (with the exception of axial flow on a cylinder by Survila and Stasiulevicius [1], as reported by Kader and Yaglom [2]). Also, the only systematic experimental study of the effect of the thermal boundary condition on heat transfer in the turbulent boundary layer known to the authors is the one by Reynolds *et al.* [3].

The experiments reported in this paper were designed to investigate the effects of the thermal boundary condition on heat transfer in the turbulent boundary layer for $Re_x \to 10^7$. All of the data is for air flow with constant free stream velocity and temperature over a smooth 2.4 m long flat plate. Cases are reported for constant temperature and constant heat flux wall boundary conditions with free stream velocities of 12, 27, 42, and 67 m s^{-1}. Linear wall temperature variations are reported for free stream velocities of 27 and 67 m s^{-1}.

The 67 m s^{-1} (Mach number ≈ 0.20) cases are on the upper fringe of incompressible flows. While the assumption of a constant air density is still a fairly good approximation, viscous dissipation must be considered for the heat transfer problem. This is discussed in some detail below. In the following section the theory of heat transfer in the turbulent boundary layer is briefly reviewed, the experimental facility is described and the results are presented, discussed, and compared with the theories.

THEORY

The theoretical treatment of heat transfer in the turbulent incompressible flat plate boundary layer flow is mature and well documented [4, 5]. Here the theory is divided into three subtopics—analogies, solutions to the integral boundary layer equations, and numerical solutions of the time averaged boundary layer equations.

Analogies

Reynolds' analogy [6] was one of the first theoretical treatments of turbulent heat transfer. For the case of constant free stream velocity and temperature, constant wall temperature, and $Pr = 1$, the similarity between the x-momentum equation and the energy equation yields

$$St = C_f/2. \tag{1}$$

The restrictions on equation (1) prohibit its wide application. Particularly troublesome is the requirement that $Pr = 1$. The two most famous extensions of the analogy for Pr of the order of 1 or greater are those of Von Karman [7] and Colburn [8].

Von Karman derived his analogy by integrating the thermal and velocity laws-of-the-wall in a three-layer model to yield

$$\frac{1}{St} = \frac{2}{C_f} + 5\sqrt{\left(\frac{2}{C_f}\right)}\{Pr - 1 + \ln[1 + 5(Pr-1)/6]\}. \tag{2}$$

Kays and Crawford [5] have shown that equation (2) can be approximated very well for gases ($0.5 < Pr < 1$) by

$$St\, Pr^{0.4} = C_f/2. \tag{3}$$

NOMENCLATURE

A	area of one test plate
a_j	piecewise linear wall temperature parameter, equation (7)
b_i	finite step in wall temperature, equation (7)
c_p	specific heat at constant pressure
c_{pa}	specific heat of dry air
c_{pw}	specific heat of water vapor
C_f	skin friction coefficient, $2\tau_w/\rho u_\infty^2$
g	kernel function in equation (10)
h	kernel function in equation (6)
H	total enthalpy, $c_p t + u^2/2$
l	Prandtl mixing length
m_j	slope in piecewise linear wall temperature variation, equation (7)
P_{bar}	barometric pressure
Pr	Prandtl number
Pr_t	turbulent Prandtl number
q_c	conduction heat loss
q_r	radiation heat loss
q''_w	heat flux at the wall
R	recovery factor
Re_x	Reynolds number, $u_\infty x/\nu$
St	local Stanton number based on total temperature
St_t	Stanton number for constant wall temperature
$\underline{t}$	temperature
$\overline{t'v'}$	turbulent heat flux factor
T	total temperature, $t + u^2/2c_p$
t_{rail}	temperature of the side rail
t_{wb}	wet bulb temperature
$\underline{u}$	x-component of time mean velocity
$\overline{u'v'}$	Reynolds shear stress factor
U_{St}	uncertainty in St (95% confidence level)
$(UA)_{eff}$	conductance, $q_c = (UA)_{eff}(t_w - t_{rail})$
v	y-component of time mean velocity
W	electric power to each plate
x	stream-wise direction
y	normal direction
y^+	non-dimensional y; $y^+ = yu_\infty\sqrt{(C_f/2)}/\nu$.

Greek symbols

α	thermal diffusivity
$\beta_\tau(a, b)$	incomplete beta function, equation (9)
$\Gamma(x)$	gamma function, $\Gamma(x+1) = x!$
δ	boundary layer thickness; defined based on $u/u_\infty = 0.99$
ε	radiative emissivity
μ	viscosity
μ_t	eddy viscosity
ν	kinematic viscosity, μ/ρ
ν_t	eddy kinematic viscosity, μ_t/ρ
ξ	unheated starting length and dummy integration parameter
ρ	density
τ	shear stress.

Subscripts

r	recovery
w	values evaluated at the wall
∞	values evaluated in the free stream.

Colburn based his analogy completely on dimensional analysis and empirical considerations. His analogy is

$$St\,Pr^{0.66} = C_f/2. \tag{4}$$

Although equation (4) was first determined by Colburn purely from empirical considerations, it has been deduced from turbulent scaling laws for $Pr > 1$ [9, 10].

Other analogies can be derived from the velocity and temperature laws-of-the-wall (Kader and Yaglom [2] for example). All of these analogies are still limited to the constant wall temperature boundary condition. However, this limitation is often not stressed and the analogies are often compared with constant heat flux experiments.

Integral analysis

For the integral analysis, we assume constant free stream velocity and temperature and a constant property fluid flow over a flat plate. For the arbitrary wall temperature or heat flux, we follow the procedure of Reynolds *et al.* [3] as presented by Kays and Crawford [5]. The procedure is to use the solution of the integral boundary layer equations for the step wall temperature with an unheated starting length as the kernel function in a superposition integral. Using the 1/7 power law approximation of the velocity and temperature profiles, Reynolds *et al.* established that for an unheated starting length, ξ, the local heat transfer coefficient can be expressed as

$$h(\xi; x) = \rho u_\infty c_p\, St_t(x)[1 - (\xi/x)^{9/10}]^{-1/9} \tag{5}$$

where $St_t(x)$ is the constant wall temperature Stanton number given by the analogy of choice from equations (1) to (4). The heat flux for a variable wall temperature, $t_w(x)$, is

$$q''_w(x) = \int_0^x h(\xi; x)\frac{d(t_w - t_\infty)}{d\xi}d\xi + \sum_{i=1}^{N} h(\xi_i; x)\Delta(t_{w,i} - t_\infty) \tag{6}$$

where $\Delta(t_{w,i} - t_\infty)$ is the ith finite step in wall tem-

perature, N the number of steps, and ξ_i are the locations of the steps.

For a piecewise linear wall temperature with a finite number of steps

$$t_w - t_\infty = \sum_{j=1}^{M} m_j(x-a_j) + \sum_{i=1}^{N} b_i \tag{7}$$

application of equation (6) with equation (5) yields

$$St(x) = \frac{10x\,St_t(x)}{9(t_w-t_\infty)} \sum_{j=1}^{M} m_j \beta_{r_j}(8/9, 10/9) + \frac{St_t(x)}{t_w-t_\infty} \sum_{i=1}^{N} b_i[1-(\xi_i/x)^{9/10}]^{-1/9} \tag{8}$$

where $\beta_{r_j}(8/9, 10/9)$ is the incomplete beta function with $r_j = 1-(a_j/x)^{9/10}$

$$\beta_r(a,b) = \int_0^r z^{a-1}(1-z)^{b-1}\,dz. \tag{9}$$

The inverse problem where the wall heat flux is specified can be formulated as

$$t_w - t_\infty = \int_0^x g(\xi; x) q_w''(\xi)\,d\xi \tag{10}$$

where

$$g(\xi; x) = \frac{9/10}{\Gamma(1/9)\Gamma(8/9)\rho u_\infty c_p\, St_t(x)\, x} \times [1-(\xi/x)^{9/10}]^{-8/9}$$

or in terms of the local Stanton number

$$\frac{1}{St(x)} = \frac{9/10}{\Gamma(1/9)\Gamma(8/9) x\, St_t(x)\, q_w''(x)} \times \int_0^x [1-(\xi/x)^{9/10}]^{-8/9} q_w''(\xi)\,d\xi. \tag{11}$$

Numerical solutions

The numerical solution of the time averaged boundary layer equations for turbulent flat plate flows is by now routine [4]. The time averaged boundary layer equations for the flow of a constant property fluid over a flat plate (constant free stream velocity and temperature) are usually reduced to

$$\frac{\partial u}{\partial x} + \frac{\partial v}{\partial y} = 0 \tag{12}$$

$$u\frac{\partial u}{\partial x} + v\frac{\partial u}{\partial y} = \nu\frac{\partial^2 u}{\partial y^2} - \frac{\partial}{\partial y}\overline{u'v'} \tag{13}$$

$$u\frac{\partial t}{\partial x} + v\frac{\partial t}{\partial y} = \alpha\frac{\partial^2 t}{\partial y^2} - \frac{\partial}{\partial y}\overline{t'v'} + \frac{1}{c_p}\left(\nu\frac{\partial u}{\partial y} - \overline{u'v'}\right)\left(\frac{\partial u}{\partial y}\right). \tag{14}$$

Before equations (12)–(14) can be solved, models for the Reynolds stress, $-\overline{u'v'}$, and the turbulent heat flux, $-\overline{t'v'}$, must be formulated. For the conditions of interest, the mixing length model and the turbulent Prandtl number concept are adequate. The models are

$$-\overline{u'v'} = \nu_t\frac{\partial u}{\partial y} = l^2\left|\frac{\partial u}{\partial y}\right|\frac{\partial u}{\partial y} \tag{15}$$

$$-\overline{t'v'} = \frac{\nu_t}{Pr_t}\frac{\partial t}{\partial y} \tag{16}$$

where

$$l = 0.4y[1-\exp(-y^+/26)]; \quad l < 0.09\delta$$

$$l = 0.09\delta; \quad \text{otherwise}$$

$$Pr_t = 0.9.$$

The boundary conditions for equations (12)–(14) are

$$x = 0: \quad u = u_\infty, \quad t = t_\infty$$

$$y = 0: \quad u = v = 0, \quad t = t_w(x) \text{ (or } q'' = q_w''(x))$$

$$y \to \infty: \quad u = u_\infty, \quad t = t_\infty. \tag{17}$$

The momentum and energy equations of the boundary layer are transformed into computational space and solved with a marching implicit finite-difference algorithm. The method is described in detail by Gatlin [11]. For all computations in this paper, the BLACOMP code as verified by Gatlin is used.

Definition of the Stanton number

The Stanton number can be defined based on the free stream total temperature, recovery temperature, or static temperature. The Stanton number data in this paper is reduced based on a definition using the total temperature

$$St = \frac{q_w''}{\rho u_\infty c_p(t_w - T_\infty)}. \tag{18}$$

The question arises as to what is the best interpretation of the Stanton number in the analogies? The usual development is to treat the analogies as applied to low speed flow where the distinction between total, recovery, and static temperature is negligible. However, for the data presented in this paper, the 67 m s^{-1} cases are on the fringe of low speed flows and the distinction between total, recovery, and static temperature makes a measurable difference in the Stanton number. At 67 m s^{-1} the difference in total and static temperature is about 2°C which is 10–13% of the nominal 20–15°C temperature difference across the boundary layer in the present experiments.

As shown in ref. [12], the definition of Stanton number based on the total temperature is consistent with Reynolds' analogy. The total enthalpy field, $H = c_p t + u^2/2$, and the velocity field, u, are similar and $St = C_f/2$ if the following conditions are met:

(1) u_∞ = constant;
(2) $Pr = Pr_t = 1$;
(3) $(H_w - H_\infty)$ = constant;
(4) the boundary conditions are similar

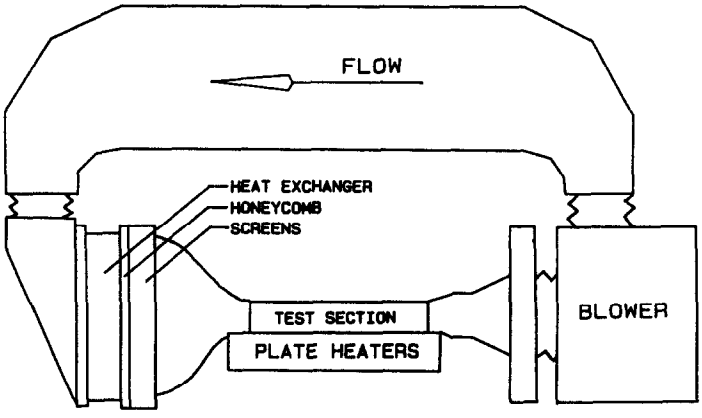

FIG. 1. Schematic of the turbulent heat transfer test facility (THTTF).

$$u(y \to \infty) = u_\infty; \quad H(y \to \infty) = H_\infty = \text{constant}$$
$$u(0) = 0; \quad H(0) = H_w = \text{constant}.$$

Therefore, it is consistent with Reynolds' analogy to define the Stanton number based on total enthalpy or temperature. In the following, the Stanton numbers for all of the analogies are taken to be defined based on total temperature. An alternate would be St based on boundary layer recovery temperature. At the modest velocities in the experiments reported here, there is very little difference in the total and boundary layer recovery temperatures.

EXPERIMENTAL APPARATUS

The experiments were performed in the turbulent heat transfer test facility (THTTF) which is shown schematically in Fig. 1. A complete description of the facility and its qualification is presented in ref. [13]. This facility is a closed loop air tunnel with a free stream velocity range of 6–67 m s^{-1}. The temperature of the circulating air is controlled with an air to water heat exchanger and a cooling water loop. Following the heat exchanger the air flow is conditioned by a system of honeycomb and screens so that the flow entering the test section is uniform and has a turbulence intensity less than 1% in all cases. The average measured turbulence intensity was 0.58% at 12 m s^{-1} and 0.42% at 42 m s^{-1}, as compared with the reported 2–3% of Reynolds *et al.* [3] and 0.7% of Kearney *et al.* [14].

The 2.4 m long test section consists of 24 electrically heated flat plates which are abutted together to form a continuous flat surface. The measured average surface roughness is less than 0.5 μm and the step between any two plates is less than 0.0125 mm. The thermal boundary condition is set by controlling the power input to each plate. The heating system is under active computer control and any desired set of thermal boundary conditions can be maintained within the limits of the power supply. For example, the plate temperature can be maintained at any temperature, ± 0.1°C, between 50°C and 2°C above the free stream air temperature which is typically 30°C. To minimize the conduction losses, the side rails which support the plates are heated to approximately the same temperature as the plates.

The top wall can be adjusted to maintain a constant free stream velocity. An inclined water manometer with a resolution of 0.06 mm is used to measure the pressure gradient during top wall adjustment. Static pressure taps are located in the side wall adjacent to each plate. The pressure tap located at the second plate is used as a reference, and the pressure difference between it and each other tap is minimized. For example, the maximum pressure difference for the 42 m s^{-1} case was 0.30 mm of water.

The boundary layer is tripped at the exit of the 19:1 area ratio inlet nozzle with a 1 mm × 12 mm wooden strip. This trip location is immediately in front of the heated surface.

Stanton number determination

The data reduction expression for the experimentally determined Stanton number is

$$St = \frac{W - q_r - q_c}{A\rho c_p u_\infty (t_w - T_\infty)}. \tag{19}$$

The power, W, supplied to each plate heater is measured with a precision wattmeter. The radiation heat loss, q_r, is estimated using a gray body enclosure model where the emissivity of the nickel plated aluminum is estimated as $\varepsilon = 0.11$. The conductive heat loss, q_c, is determined using an experimentally determined plate to side rail conductance, $(UA)_{eff}$. The conduction losses are minimized by actively heating the side rails. The plate area, A, is determined from the length and width dimensions. The density and specific heat are determined from property data for moist air using the measured values of barometric pressure and wet and dry bulb temperatures in the

Table 1. Estimated bias limits at 95% confidence

W	0.9%
t_w	0.14°C
t_r	0.1°C
t_{rail}	0.4°C
t_{wb}	0.6°C
ε	45%
$(UA)_{eff}$	45%
R	0.09
P_{bar}	1 mm Hg
A	0.03%
u_∞	0.4%
c_{pw}	0.5%
c_{pa}	0.5%

tunnel. The free stream velocity is measured using a pitot probe and specially calibrated precision pressure transducers. The free stream and plate temperatures are measured using specially calibrated thermistors. The free stream total temperature, T_∞, is computed using a recovery factor for the free stream thermistor probe of $R = 0.86$ [15]. The experimentally determined Stanton number is then a function of the 13 measured variables and reference parameters

$$St = St(W, \varepsilon, A, t_w, t_r, t_{rail}, (UA)_{eff}, t_{wb}, P_{bar}, c_{pa}, c_{pw}, u_\infty, R). \quad (20)$$

The uncertainty in the experimentally determined Stanton number was estimated based on the ANSI/ASME Standard on Measurement Uncertainty [16]. Precision errors associated with all measured variables used to determine the Stanton number were found to be negligible compared with the corresponding bias errors. The bias limits in the measured variables and the input parameters were estimated, and the uncertainty in the Stanton number was computed using the procedures outlined in the standard. Since all of the thermistors were calibrated against the same standard, some elemental contributions to the thermistor bias limits were correlated. This was taken into account in the uncertainty analysis. The bias limit estimates (at 95% confidence) for the individual measurements are given in Table 1. Table 2 gives typical values for Stanton number uncertainty under representative conditions for constant wall temperature. Complete listings of the uncertainties can be found in refs. [12, 13].

An additional source of uncertainty for the cases without a constant wall temperature is the plate to plate conductance. The plates are trimmed to touch on a lip of about 1.6 mm thickness. Based on calibration experiments the plate to plate conductance was found to be 1.25 W °C^{-1}. For the linear wall temperature variations, the net effect of plate to plate conductance is small because about the same heat enters each plate from the high temperature side as leaves from the low temperature side. The exception to this are the points where the linear variation changes slope. These points are all noted when the data is presented. The constant heat flux cases do not have linear wall temperature variation. This effect was investigated for all constant heat flux cases. It was observed that beyond the eighth plate the wall temperature variations were very small and the plate to plate conduction was negligible. For the first eight plates an additional 1% should be added to the Stanton number uncertainty for the constant heat flux cases. For example, the uncertainty in St at plate 8 for $u_\infty = 12$ m s^{-1} increased from $U_{St} = 3.6$ to 4.6%. Therefore, the plate to plate conduction has a very small effect on the Stanton number.

Table 2. Stanton number uncertainties for typical cases (constant wall temperature; at plate 15)

u_∞ (m s^{-1})	67.2	42.9	27.9	12.4
U_{St}/St (%)	3.1	1.7	1.7	3.7
St	0.00145	0.00156	0.00166	0.00196
W (W)	61.37	61.50	45.04	24.40
q_r (W)	0.41	0.597	0.597	0.605
q_c (W)	−0.614	0.638	−0.234	0.092
t_w (°C)	44.0	47.8	44.0	44.0
T_∞ (°C)	32.5	31.1	26.5	26.2

Skin friction measurement

The skin friction coefficient, C_f, was determined using a 3 mm diameter Preston tube. The calibration equations given by Patel [17] were used to determine C_f from the Preston tube pressure measurement. The uncertainty in the C_f measurements is estimated to be less than ±6% at 95% confidence. All C_f measurements were made in an isothermal boundary layer.

RESULTS AND DISCUSSION

Stanton number data were taken for both constant wall temperature and constant heat flux boundary conditions for nominal free stream velocities of 12, 27, 42, and 67 m s^{-1}. The experiments were conducted so that the constant heat flux cases had approximately the same wall temperature far from the boundary layer origin as the corresponding constant wall temperature cases. These data are compared with the analogies, the integral solutions, and the numerical solutions of the boundary layer equations. However, the primary comparison is the comparison of the data sets with each other. In addition, Stanton number data are presented for a linear wall temperature distribution with free stream velocities of 27 and 67 m s^{-1}. Comparisons are made between these data and the integral solutions and numerical solutions. Tabular data for all cases can be found in refs. [12, 13].

For the experimental results and all of the computations, the origin of the momentum boundary layer was taken to be the nozzle exit, and the origin of the thermal boundary layer was taken to be the start of the heated surface. These points were coincident for all the cases reported in this paper. The authors decided not to include any virtual origin estimates in the data presentation or computations. The experimental data and all of the computations were based

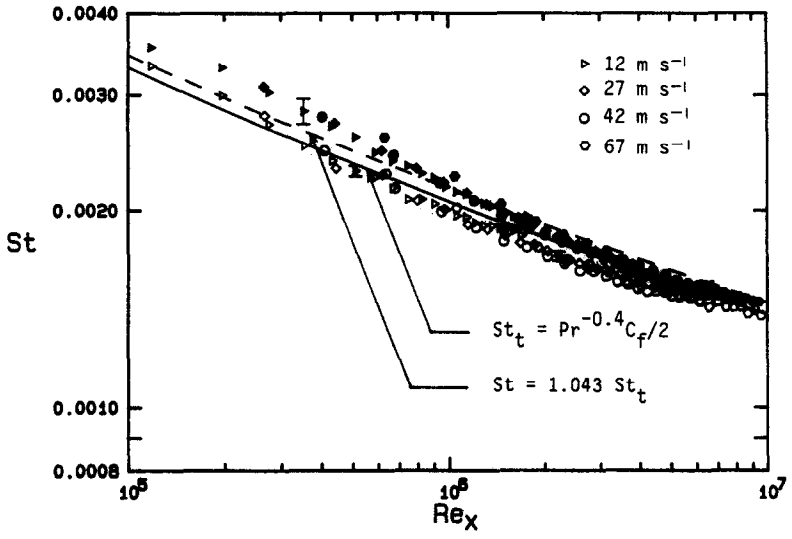

FIG. 2. Stanton number results for constant wall temperature (open symbols) and constant wall heat flux (solid symbols).

on constant properties which were evaluated at the free stream static temperature.

Constant q''_w vs constant t_w

Figure 2 presents a plot of St vs Re_x for the two boundary conditions. The solid symbols are the results for the constant heat flux boundary condition and the open symbols are for the constant wall temperature boundary condition. The solid curve is the analogy of equation (3), $St\,Pr^{0.4} = C_f/2$, where the skin friction coefficient is determined using the Schultz-Grunow [18] correlation

$$C_f/2 = 0.185[\log_{10}(Re_x)]^{-2.584} \qquad (21)$$

The figure shows that the analogy fits the constant wall temperature data very well for the Reynolds number range 100 000–10 000 000. At the maximum deviation the correlation is about 5% too high. The dashed curve is based on the integral solution, equation (11), for the case of constant q''_w

$$St = \frac{\Gamma(1/9)\Gamma(8/9)}{\beta_1(1/9, 10/9)} St_t = 1.043 St_t. \qquad (22)$$

In the far boundary layer, equation (22) agrees almost exactly with the data. For Reynolds numbers between 3 000 000 and 10 000 000, the constant wall heat flux data are consistently 4–5% greater than the constant wall temperature data. However, near the origin of the boundary layer the constant wall heat flux data are 10–15% above the constant wall temperature data.

The two boundary conditions are compared more directly in Fig. 3. The ratio of constant wall heat flux to constant wall temperature Stanton numbers is plotted directly. The dashed curve represents the integral solution, equation (22), and the solid lines represent the numerical solutions of the boundary layer equations. For Reynolds numbers greater than 3 000 000, the data agree very closely with equation (22). But, for the low Reynolds numbers, the data indicate a ratio of 1.10–1.15 instead of 1.04. The numerical solutions agree with the data for all of the Reynolds numbers. The numerical solutions indicate a slight unit Reynolds number effect which is perhaps suggested by the data but not proven.

The integral solution is based on the very approximate 1/7 power law velocity and temperature profiles. Therefore, it should be viewed as an asymptotic case where the boundary layer has had a chance to develop well. The degree of success demonstrated here should be considered as an indication of the power of the integral solution.

As stated above, Reynolds' analogies strictly apply only for the constant wall temperature boundary condition. However, they are also considered to apply approximately for the constant heat flux boundary condition. Constant wall heat flux data are often reported in terms of the Reynolds analogy factor, $2St/C_f$ (for example, Subramanian and Antonia [19], and Simonich and Bradshaw [20]). In Fig. 4 the data are presented in analogy coordinates, $2St/C_f$, directly. Again the solid symbols are the constant q''_w results and the open symbols are the constant t_w results. The skin friction coefficients are the values measured with a Preston tube. The dashed lines are, as indicated, the Colburn analogy, $Pr^{-0.66}$, and the approximation of Von Karman's analogy, $Pr^{-0.4}$. The solid lines represent the results from the numerical solutions. The analogy factors for the constant t_w data are more or less constant for the whole Reynolds number range. The data scatter about the value of about 1.2 which is approximately halfway between the two analogies. The numerical solutions for the constant t_w case are

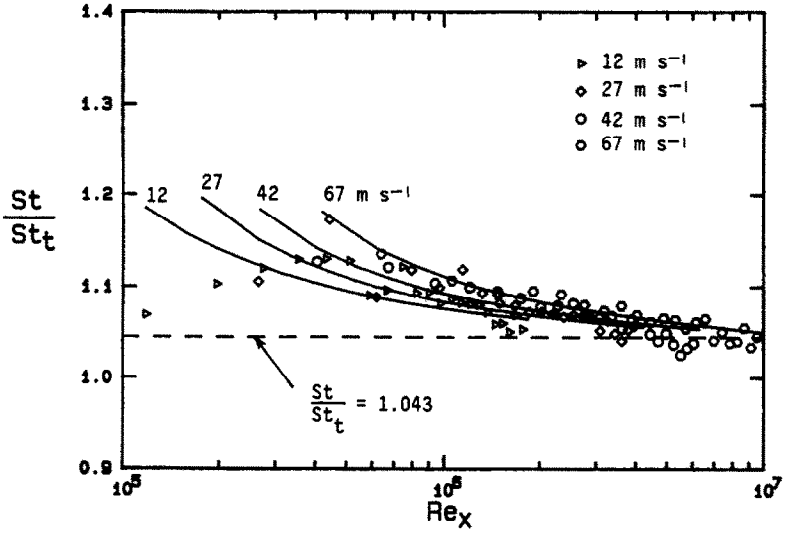

FIG. 3. Direct comparison of constant q''_w and constant t_w thermal boundary conditions.

in very good agreement with the data; they are practically constant at $2St/C_f = 1.18$–1.2 and show only a small unit Reynolds number effect. The analogy factors for the constant q''_w boundary condition show a Reynolds number dependence. The ratio decreases from about 1.4 at low Reynolds numbers to about 1.24 at higher Reynolds numbers. The numerical solutions are in good agreement with the data, and show a small unit Reynolds number effect. Simonich and Bradshaw [20], and Subramanian and Antonia [19] present limited heat transfer data for turbulent boundary layers with constant q''_w boundary conditions. Simonich and Bradshaw found that $2St/C_f$ varied between 1.3 at low Reynolds numbers to 1.2 at $Re_x = 3\,500\,000$. Subramanian and Antonia found $2St/C_f$ to vary from 1.5 at low Re_x to 1.4 at $Re_x = 3\,000\,000$. These results are in substantial agreement with the present results.

Linear wall temperatures

Experiments were conducted using a linear wall temperature boundary condition at free stream velocities of 27 and 67 m s^{-1}. The measured wall temperatures are shown in Fig. 5. The first five plates were heated to 50°C and the temperature was allowed to drop by 0.5°C for each of the following plates. Each plate is 101.6 mm wide in the flow direction. The results from these experiments are compared with the integral solutions and the numerical solutions. The integral solutions are given by equations (7) and (8). Also, in light of the discussion on Stanton number and free stream

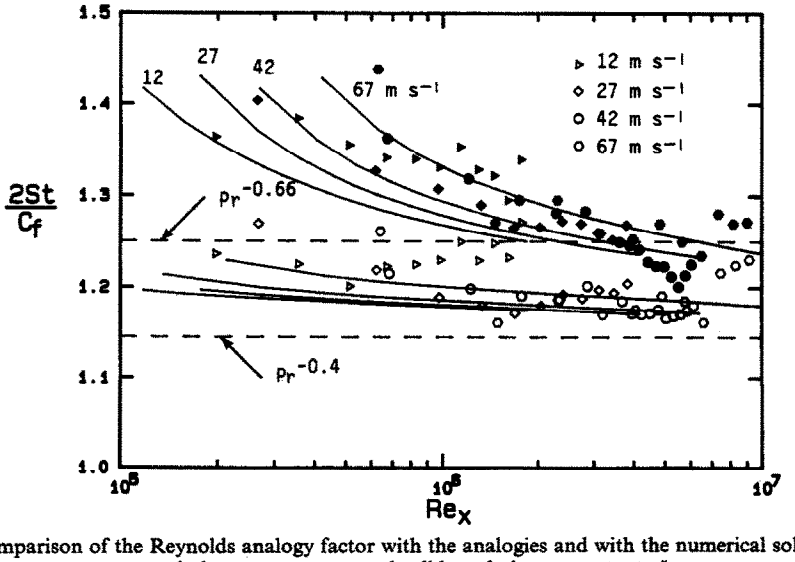

FIG. 4. Comparison of the Reynolds analogy factor with the analogies and with the numerical solutions; open symbols are constant t_w and solid symbols are constant q''_w.

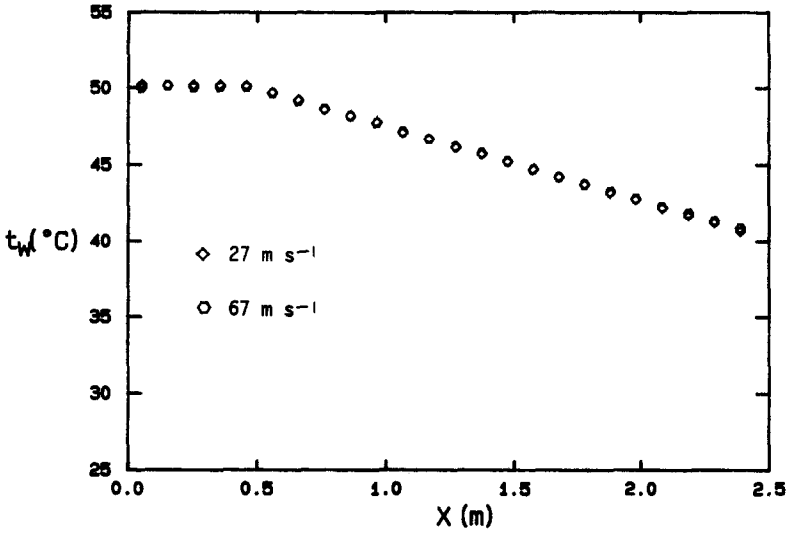

FIG. 5. Wall temperature variations.

total temperature, the total temperature, T_∞, is used in equations (7) and (8).

Figures 6 and 7 show the data and comparisons with the integral and numerical solutions for the case with linear wall temperature variation for stream velocities of 27 and 67 m s^{-1}, respectively. The dashed curve represents the integral solution and the solid curve the numerical solution. The solid symbols represent the data for the plates with a discontinuity in wall temperature slope. The data in these figures are presented in terms of the ratio of local Stanton number to constant wall temperature Stanton number, St/St_t. This is the natural form of the integral solutions and allows direct comparison without the corrupting influence of one of the correlations for St_t. The numerical computations were made at the same free stream conditions for both St and St_t, so that the unit Reynolds number is the same for each condition. The figures show that the two solutions are in substantial agreement with the data. The numerical solutions predict a slightly more rapid decrease in the Stanton number than the integral solution.

SUMMARY

Experimental results are presented and compared with the theories for a variety of thermal boundary conditions—constant wall temperature, constant wall heat flux, and a linear wall temperature variation. The Stanton number data extend the Reynolds number range from the 3 500 000 of Reynolds *et al.* [3] to 10 000 000. The constant wall temperature Stanton

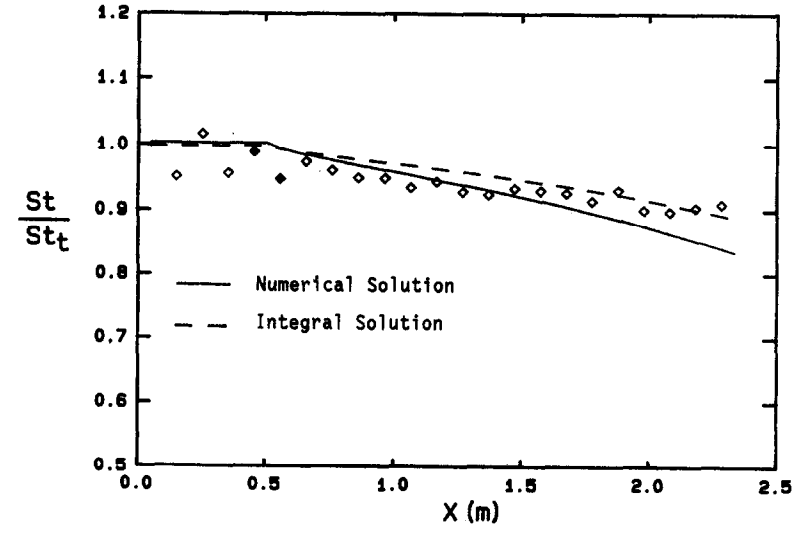

FIG. 6. Stanton number results for the linear wall temperature variation with $u_\infty = 27.6$ m s^{-1}, $T_\infty = 27.5$°C.

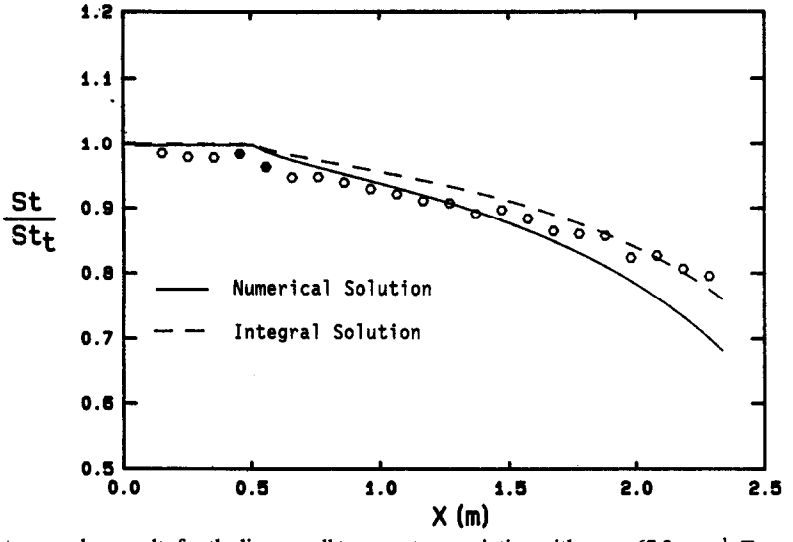

FIG. 7. Stanton number results for the linear wall temperature variation with $u_\infty = 67.2\,\mathrm{m\,s^{-1}}$, $T_\infty = 34.8°\mathrm{C}$.

number data are found to be in reasonable agreement with the Von Karman analogy over the entire Reynolds number range when the skin friction coefficient is taken from the Schultz-Grunow correlation. A measurable difference of 5–15% is found between Stanton number for the constant wall temperature and constant wall heat flux. The Reynolds analogy factor, $2St/C_f$, is more or less constant at about 1.2 for the constant wall temperature cases; however, the constant heat flux data show a Reynolds number dependence for $2St/C_f$. Both the integral solutions and the numerical solutions are found to be in substantial agreement with the linear wall temperature variation cases.

Acknowledgement—This work was supported by the U.S. Air Force Office of Scientific Research (Research Grant AFOSR-86-0178). The interest and encouragement of Dr Jim Wilson and Capt. Hank Helin are gratefully acknowledged. The experimental apparatus was acquired under Grant AFOSR-85-0075.

REFERENCES

1. V. Survila and Y. Stasiulevicius, Heat transfer of a longitudinally streamlined cylinder having an artificial turbulization of the approaching boundary layer, *Trudy Akad. Nauk. Lit. SSR* **2B**, 113–121 (1969).
2. B. A. Kader and A. M. Yaglom, Heat and mass transfer laws for fully turbulent wall flows, *Int. J. Heat Mass Transfer* **15**, 2329–2351 (1972).
3. W. C. Reynolds, W. M. Kays and S. J. Kline, Heat transfer in the turbulent incompressible boundary layer, Parts I, II, and III, NASA MEMO 12-1-58W, 12-2-58W, and 12-3-58W, Washington, DC (1958).
4. T. Cebeci and P. Bradshaw, *Physical and Computational Aspects of Convective Heat Transfer*. Springer, New York (1984).
5. W. M. Kays and M. E. Crawford, *Convective Heat and Mass Transfer*. McGraw-Hill, New York (1980).
6. O. Reynolds, On the extent and action of the heating surface for steam boilers, *Proc. Manchr Lit. Phil. Soc.* **14**, 7 (1874).
7. Th. Von Karman, The analogy between fluid friction and heat transfer, *Trans. ASME* **61**, 705–710 (1939).
8. A. P. Colburn, A method of correlating forced convection heat transfer data and a comparison with fluid flow, *Trans. Am. Inst. Chem. Engrs* **29**, 174–210 (1933).
9. A. Bejan, *Convective Heat Transfer*. Wiley, New York (1984).
10. V. S. Arpaci and P. S. Larsen, *Convective Heat Transfer*. Prentice-Hall, Englewood Cliffs, New Jersey (1984).
11. B. Gatlin, An instructional computer program for computing the steady, compressible, turbulent flow of an arbitrary fluid near a smooth wall, M.S. Thesis, Mechanical and Nuclear Engineering Department, Mississippi State University (1983).
12. P. Love, R. P. Taylor, H. W. Coleman and M. H. Hosni, Effects of thermal boundary condition on heat transfer in the turbulent incompressible flat plate boundary layer, TFD-88-3, Mechanical and Nuclear Engineering Department, Mississippi State University (1988).
13. H. W. Coleman, M. H. Hosni, R. P. Taylor and G. B. Brown, Smooth wall qualification of a turbulent heat transfer test facility, TFD-88-2, Mechanical and Nuclear Engineering Department, Mississippi State University (1988).
14. D. W. Kearney, R. J. Moffat and W. M. Kays, The turbulent boundary layer: experimental heat transfer with strong favorable pressure gradients and blowing, Report No. HMT-12, Department of Mechanical Engineering, Stanford University (1970).
15. R. G. Eckert and R. J. Goldstein, *Measurements in Heat Transfer* (2nd Edn). McGraw-Hill, New York (1976).
16. Measurement uncertainty, ANSI/ASME PTC 19.1–1985, Part 1 (1986).
17. V. C. Patel, Calibration of the Preston tube and limitations on its use in pressure gradients, *J. Fluid Mech.* **23**, 185–208 (1965).
18. F. Schultz-Grunow, New frictional resistance law for smooth plates, NACA TM986, Washington, DC (1941).
19. C. S. Subramanian and R. A. Antonia, Effect of Reynolds number on a slightly heated turbulent boundary layer, *Int. J. Heat Mass Transfer* **24**, 1833–1846 (1981).
20. J. C. Simonich and P. Bradshaw, Effect of free-stream turbulence on heat transfer through a turbulent boundary layer, *J. Heat Transfer* **100**, 671–677 (1978).

EFFETS DES CONDITIONS AUX LIMITES THERMIQUES SUR LE TRANSFERT DE CHALEUR DANS UNE COUCHE LIMITE TURBULENTE ET INCOMPRESSIBLE SUR PLAQUE PLANE

Résumé—On présente des résultats expérimentaux pour le nombre de Stanton en couche limite turbulente et incompressible sur plaque plane avec une variété de conditions aux limites thermiques: température constante à la paroi, flux thermique pariétal constant et variation linéaire de température pariétale. Ces expériences s'étendent jusqu'à un nombre de Reynolds Re_x de 10 000 000. La condition aux limites thermique a une influence significative sur le nombre de Stanton. Les résultats expérimentaux sont comparés avec différentes théories d'analogie avec le frottement pariétal, des solutions des équations intégrales de couche limite, et des solutions aux différences finies des équations aux dérivées partielles moyennes de couche limite.

EINFLUSS DER THERMISCHEN RANDBEDINGUNGEN AUF DEN WÄRMETRANSPORT IN DER TURBULENTEN, INKOMPRESSIBLEN GRENZSCHICHT AN EINER PLATTE

Zusammenfassung—Es werden experimentell ermittelte Stanton-Zahlen für die turbulente inkompressible Grenzschicht an einer Platte für einige thermische Randbedingungen—isotherme Wand, konstante Wärmestromdichte und linearer Temperaturverlauf in der Wand—vorgestellt. Bei diesen Experimenten wurden Reynolds-Zahlen bis 10 000 000 erreicht. Die thermische Randbedingung hat dabei einen wesentlichen Einfluß auf das Verhalten der Stanton-Zahl. Die experimentellen Ergebnisse werden mit verschiedenen Theorien zum Wärmetransport verglichen—Analogie zum Druckverlust, Lösung der integralen Grenzschichtgleichungen und Lösung der nach Reynolds gemittelten Grenzschichtgleichungen mittels des Finite-Differenzen-Verfahrens.

ВЛИЯНИЕ ГРАНИЧНЫХ УСЛОВИЙ НА ТЕПЛОПЕРЕНОС В ТУРБУЛЕНТНОМ НЕСЖИМАЕМОМ ПОГРАНИЧНОМ СЛОЕ НА ПЛОСКОЙ ПЛАСТИНЕ

Аннотация—Представлены экспериментальные результаты для числа Стэнтона в случае турбулентного несжимаемого пограничного слоя на плоской пластине с различными граничными условиями—постоянной температурой стенок, постоянным тепловым потоком на стенках и линейно изменяющейся температурой стенок. Эксперименты расширили диапазоны разультатов для таких условий переноса тепла до числа Рейнольдса 10^7. Найдено, что тепловое граничное условие оказывает значительное влияние на характер числа Стэнтона. Экспериментальные данные сравниваются с результатами различных теорий теплопереноса в пограничном слое, с решениями интегральных уравнений пограничного слоя и конечно-разностными решениями уравнений пограничного слоя, усредненных по Рейнольдсу.